International
Collaboration
Center
Institute for Materials Research
Tohoku University
ICC-IMR

ICC-IMR FY2013
Activity Report

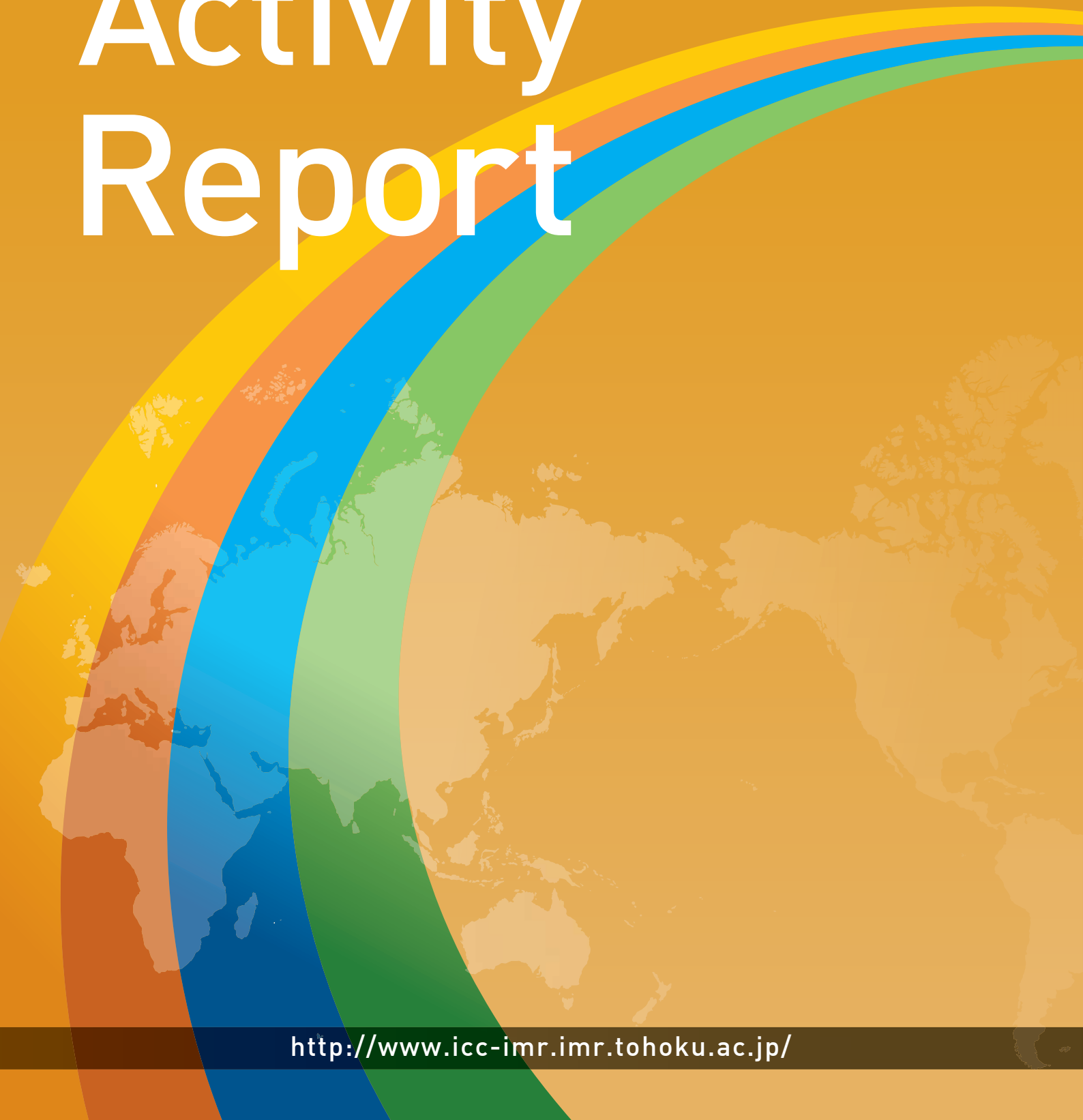

http://www.icc-imr.imr.tohoku.ac.jp/

ICC-IMR FY2013

Activity Report

International Collaboration Center

Institute for Materials Research
Tohoku University

CONTENTS

Mission

The ICC-IMR was founded in April 2008 as the center for international collaboration of the Institute for Materials Research (IMR) a center of excellence in material science, consisting of 27 research groups and five research centers. The ICC-IMR works as a gateway of diverse collaborations between overseas and IMR researchers. The ICC-IMR has invited 34 visiting professors and conducted 16 international research projects since its start-up (please inspect the graph below for more details,). The applications are open to foreign researchers and the projects are evaluated by a peer-review process involving international reviewers.

ICC-IMR coordinates six different programs:

1) International Integrated Project Research
2) Visiting Professorships
3) Short Single Research Visits
4) International Workshops
5) Fellowship for Young Researcher and PhD Student
6) Material Transfer Program

We welcome applicants from around the globe to submit proposals!

Visitors supported by ICC-Programs.

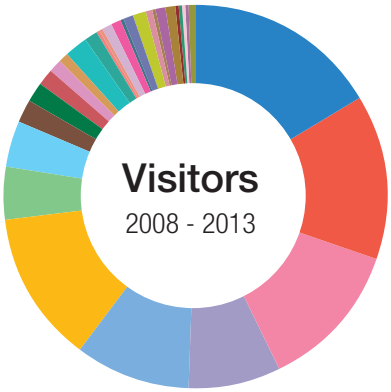

USA	50	Singapore	3	Norway	3
China	43	India	6	Ukraine	2
Korea	38	Italy	3	Turkey	1
UK	24	Argentina	1	Australia	1
France	29	Belgium	1	Austria	1
Germany	39	Slovenia	2	Slovakia	1
Netherlands	14	Spain	3	Czech Republic	1
Russia	12	Thailand	1		
Switzerland	6	Poland	2		
Iran	5	Taiwan	4		
Canada	4	Vietnam	1		
Mexico	3	Hong-Kong	1		

ICC-IMR COMMITTEE MEMBERS

Director

Prof. Hiroyuki NOJIRI

Steering Committee

Prof. Takashi GOTO

Prof. Koki TAKANASHI

Prof. Shin-ichi ORIMO

Prof. Eiji SAITOH

Prof. Gerrit E. W. BAUER

Prof. Hitoshi MIYASAKA

Activity Report

Visiting Scholars

FY 2013 Visiting Scholars

No.	Candidate	Host	Proposed Research	Title	Affiliation	Term
13G1	Burak Dikici	M. Niinomi	Investigation of Eectrochemical Biocompatibilities of β -type Ti-Nb-Ta-Zr and Co-Cr-Mo Alloys Through Microstructural Refinement	Assoc. Professor	Yuzuncu Yil University, Turkey	2013.7.3-8.14
13G2	Atsufumi Hirohata	K. Takanashi	Experimental Demonstration of a Persistent Current	Reader	University of York, UK	FY2013
13G3	Timothy Ziman	H. Nojiri	Transport and Non-Linear Correlation Functions in Frustrated Metallic Antiferromagnets	Research Director (CNRS) and Head of the Theory Group (ILL)	CNRS and Institut Laue Langevin, France	FY2013
13G4	Christian Schröder	H. Nojiri	Large Scale Simulations of Hybrid Nano-Magnetic Systems, Molecular Based Magnets, Magnetic Multi-Layers and Their Composites	Professor	University of Applied Sciences Bielefeld, Germany	FY2013
13G5	Vladimir Kochurikhin	A. Yoshikawa	Development of Growth Technology for Large Size Bulk and Shaped Growth on Scintillator, Piezo-Electric and Halogen Single Crystals	Head of Laboratory	General Physics Institute, Russian Academy of Sciences, Russia	2013.11.5-12.5
13G6	Carl Boehlert	M. Niinomi	Analysis of Deformation Behavior of Beta-Type Titanium Alloys for Biomedical Applications	Assoc. Professor	Michigan State University, USA	2014.1.6-2.6

Investigation of electrochemical biocompatibilities of beta-type Ti-Nb-Ta-Zr and Co-Cr-Mo alloys through microstructural refinement

We aimed to investigate the electrochemical behaviours of *β* type Ti-Nb-Ta-Zr (TNTZ) and Co-Cr-Mo (CCM) alloys in this collaboration. *In-vitro* corrosion susceptibilities of the alloys were compared with traditional implant materials such as Ti-6Al-4V and CP Ti in this study. Also, the effect of high-pressure torsion (HPT) on the corrosion susceptibilities of the alloys was investigated in simulated body fluid.

Metallic materials are used as biomedical implants for various parts of the human body for many decades. The physiological environment (body fluid) is considered extremely corrosive to metallic surfaces and corrosion is one of the major problems to the widespread use of the metallic materials in the human body because the corrosion products can cause infections, local pain, swelling, and loosening of the implants.

Recently, the most common corrosion resistant metallic biomaterials are made of stainless steels, titanium (Ti) and its alloys and cobalt (Co)-chromium (Cr)-molybdenum (Mo) alloys. Ti and Co alloys are the most common biomaterials because of their well chemical, mechanical and biocompatibility characteristics. Ti alloys are known for its high corrosion resistant due to instant formation of an inert oxide layer on its surface and chromium oxides increase the corrosion resistance of Co-Cr-Mo alloys.

During the visiting period, in-vitro corrosion susceptibilities of β-type Ti-Nb-Ta-Zr (TNTZ) and Co-Cr-Mo (CCM) alloys were compared with commercial implant materials such as Ti-6A-4V, and commercially pure Ti (CP Ti). The high-pressure torsion (HPT) processing is a well-proved technique for metallic materials to form ultrafine grained or/and nanostructures [1-2]. Therefore, the effect of HPT on the corrosion susceptibilities of TNTZ and CCM alloys were also investigated under *in-vitro* conditions at body temperature.

Potentiodynamic scanning (PDS) plots for the studied samples in Ringer's solution are shown in Fig. 1. The PDS profiles of the samples are quite similar each other and, all samples reach their respective stable passive current densities as the potential increases. The passive current densities remain almost unchanged inside their

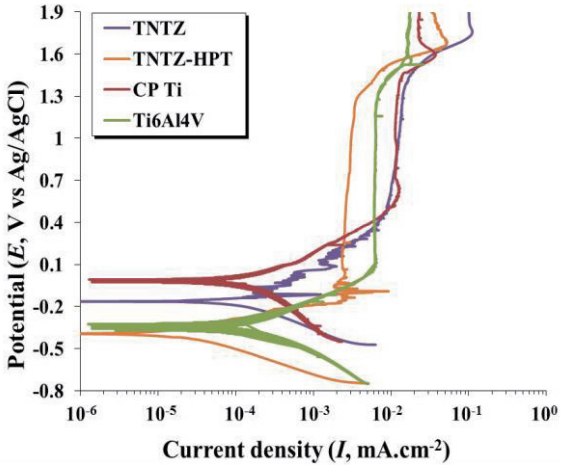

(a) Ti alloys

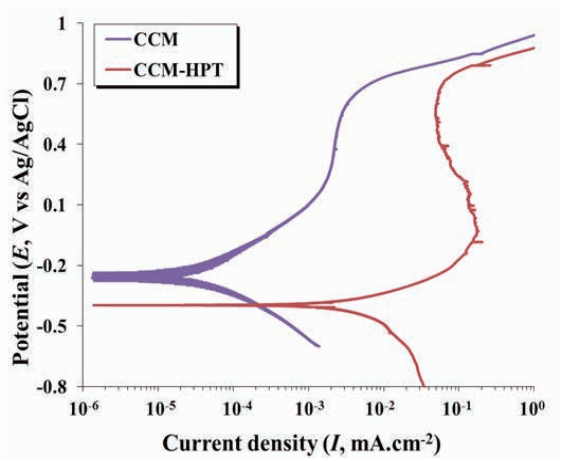

(b) Co alloys

Fig. 1 Potentiodynamic polarization curves of (a) Ti alloys and (b) Co alloys

wide passive regions, indicating that their corrosion rates are in steady state and the passive films formed on the surfaces are stable.

These results indicate that the severely strained TNTZ (TNTZ-HPT) is more resistant to corrosion than the other Ti counterparts in Ringer's solution. In addition, TNTZ-HPT shows lower E_{pp} (passivation potential) value and a wider passivation range as compared to the others. Since the supersaturated solid solution

decomposes completely and reaches the equilibrium state after the HPT. Therefore, the protective oxide layer on the surface of TNTZ-HPT is less complex or better when compared with the others. This behavior is related to its small current density and width passive area as shown in Fig. 1. (a). It can be concluded from above results that the HPT can be considered to give a balance between deformation-induced disordering and deformation-accelerated diffusion towards the equilibrium state in the Ti based alloys.

As seen from Fig. 1 (b), the corrosion potential (E_{corr}) of the CCM sample is more noble than CCM-HPT. This is in contradiction with the obtained results for Ti based alloys (Fig. 1 (a)) in this study. In other words, the electrochemical behavior of the CCM alloys is different from that of Ti alloys. The behavior may be related to increasing crystal defects, high dislocation density, grain size and crystal orientation, and residual stress after the HPT in the sample. In addition, this relates to passive film formed on their surfaces. Since the stability of passive oxide film of the TNTZ alloys is higher than that of the CCM alloys.

It is well known that protective surface films the surfaces of the alloys play key role in corrosion of the metallic implants [3-5]. TNTZ alloys have a large potential range, nobler positive potentials and lower current density values than CCM alloys due to both transpasivation and oxygen evolution reaction. It can be said that oxide layer formed on the TNTZ alloys is more stable, less soluble and more biocompatible compared to chromium oxide based layer formed on the CCM alloys.

In the view of the HPT, there is no general rule for corrosion resistance of the alloys. That they may corrode either very quickly (for CCM) or extremely slowly (for TNTZ) is mainly related to its thermo-mechanical past and medium characteristics.

Clearly, the results of the mechanical and corrosion behaviors show that there is a strong connection between corrosion resistance and microstructural features of the metallic materials, including grain diameter and states of grain boundary and secondary phases. However, further systematic approach is needed to using in human bodies of the severe deformed structure.

I am very much appreciate the fact that Prof. Mitsuo Niinomi and his research group invested their valuable time and effort to the research sharing with me their views and suggestions based on their experiences. I hope that our near future collaboration continues.

References

[1].M. Niinomi, J. Mech. Behav. Biomed. Mater. 1, 30-42 (2008).
[2].Dikici, B., Yilmazer H., Niinomi M., Nakai M., Ozdemir I., Gavgali M., Physico Chemical Mechanics of Materials, Special Issue No: 9, 95-100, 4-6 (2012).
[3].Esen Z., Dikici B., Duygulu Ö., Dericioğlu A. F., Mater Sci and Eng A, 573, 119-126 (2013).
[4].Uhlig Herbert, H., Corrosion and Corrosion Control, John Wiley&Sons Inc., U.S.A-Canada, 185-205/334-350 (1963).
[5].N. T. C. Oliveira, A. C. Guastaldi, Acta Biomater. 5, 399-405 (2009)

Keywords: Metallic biomaterials; β- type titanium alloys; High-pressure torsion; Corrosion
Full Name: Dr. Burak Dikici (Yuzuncu Yil University, Department of Mechanical Engineering, Van-Turkey)
E-mail: burakdikici@yyu.edu.tr
http://www.yyu.edu.tr/
http://www.burakdikici.com

Experimental Demonstration of a Persistent Current

By combining an epitaxial FePt nanopillar with perpendicular magnetic anisotropy and a non-magnetic nanoring, we will demonstrate an alternative method to generate a spin-polarised persistent current in a non-magnet. Even though such a spin-polarised persistent current has been proposed theoretically almost 20 years ago [1], there has been no experimental demonstration to date. This device would open up new horizon as a spin source for quantum computation.

Quantum phases of charged particles have been investigated in mesoscopic structures, and have revealed interference and oscillatory behavior induced by an external field application [2]. For instance, electrons travelling along semiconductor or normal metal rings threaded by a magnetic flux acquire a quantum dynamical phase, producing interference phenomenon such as the Aharonov-Bohm (AB) and Altshuler-Aronov-Spivak (AAS) effects. In addition, when the spin of electron rotates during its orbital motion along the ring-shaped path, the electron acquires an additional phase contribution known as the geometrical or Berry phase.

Recently, a geometrical phase has been predicted by studying electron transport under an inhomogeneous magnetic field. The geometrical phase can drive a persistent current. A pioneering experiment has been performed using spin-orbit scattering in a two-dimensional electron gas (2DEG) semiconductor, which also strongly couples spin and orbital motion and introduces a spin rotation. For metallic rings, it has been pointed out that electrons can sense the geometrical phase even when an effective exchange field is induced by ferromagnets. However, no results have been reported on the correlation between the geometrical phase and the presence of the ferromagnets. Interestingly, as opposed to a general belief that ferromagnets destroy quantum phase effects due to their complex dephasing mechanisms, an oscillatory behavior of resistance in a permalloy nanoring has been observed and an effect of ferromagnetic ordering in a GaMnAs semiconductor has been detected experimentally [3]. Such an AB oscillation in a ferromagnetic ring has been studied theoretically, suggesting that a dynamic phase can exist under the special condition when a ferromagnetic ring possesses perpendicular anisotropy. I have previously explored the effect of ferromagnets upon the electron quantum phase using a metallic nanoring, consisting of a trilayered FeNi/Cu/FeNi structure known as a current-in-plane (CIP) giant magnetoresistive (GMR) spin valve [4].

Previously we have fabricated FePt nanopillar encircled by a Au nanopillar. At 350 mK, significant hysteresis was observed in the magnetoresistance when the magnetisation of the pillar was measured [5]. The stray field from the pillar will act at a slight angle to the nanoring because the two objects do not lie in exactly the same plane. This will induce a persistent current in the ring. The simple 4-terminal configuration then allows the persistent current to be detected. The persistent current was observed via the hysteresis in the magnetoresistance when the magnetisation of the pillar was measured.

We have further improved a new nanofabrication method has been successfully developed to produce a quantum device on a MgO(001) substrate consisting of a 300-nm-inner-diameter non-magnetic nanoring and a 70-nm-diameter FePt nanopillar inside by using electron-beam lithography and Ar-ion milling. The nanoring is 100 nm wide with 15 nm Cr and 5 nm Au layers to improve the adhesion onto the MgO substrate. As shown in Fig. 1, the center nanopillar is designed to provide a non-uniform magnetic field in the nanoring at its remanent state after perpendicular saturation. Such a non-uniform field is theoretically expected to induce a persistent spin current in the nanoring [1]. The induced current is intended to be measured by four contacts fabricated near the nanoring.

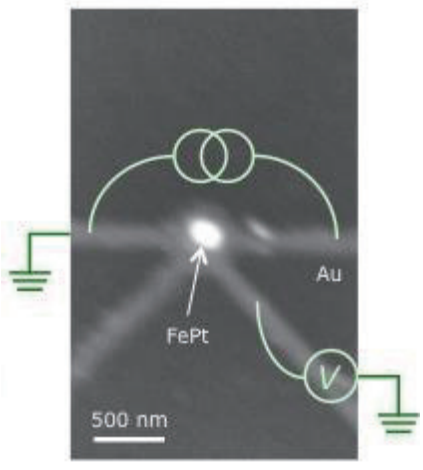

Fig. 1 SEM image of the device measured.

We introduced a constant current of 150 nA using three-terminal geometry to observe new quantum phenomena. The measurements were carried out at Prof. Kobayashi's group in Osaka University using their dilution refrigerator (Oxford

Instruments, MX Kelvinox400) at a temperature range between 25 mK and 5.0 K under magnetic fields within ±1 T. A combination of a lock-in amplifier (Stanford, SR830), low-noise pre-amplifier (NF, LI-75A) and a standard resistance (2 MΩ) was used to improve signal-to-noise ratios. We will first detect the observation of the AB signals to confirm the quality of the devices. Accordingly, we will focus on a persistent current induced in a non-magnetic nanoring under a non-uniform magnetic field application as predicted in Ref. [1].

Figure 2 shows magnetoresistance curves measured at 25 mK. A clear oscillation is observed at the period of 80~100 mT, which is larger than that estimated from the nanoring diameter (20~60 mT). This may be caused by the presence of multiple electron paths or universal conductance fluctuation within 100-nm-wide nanoring. Under the non-uniform magnetic fields generated by the FePt nano-pillar, the Berry phase is induced, resulting shifts in the AB oscillation. Such shits are sensitive to the directions of the non-uniform fields and are expected to be hysteretic. However, our measured magnetoresistance shows no hysteresis and indicate that the Berry phase is not detected at this stage.

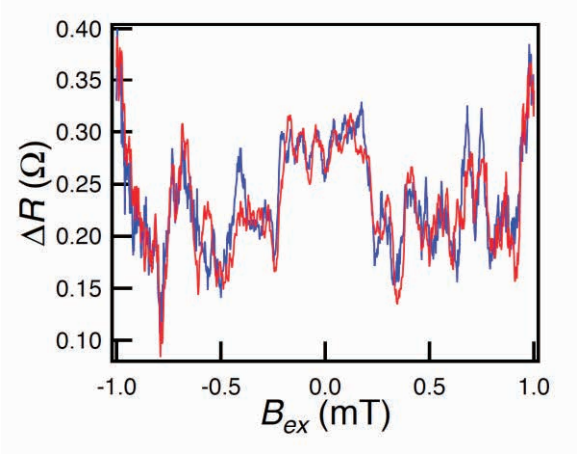

Fig. 2 Magnetoresistance measured at 25 mK with increasing (blue) and decreasing (red) an applied magnetic field.

Around zero field, symmetric increase in the magnetoresistance was observed with increasing field as a proof of weak anti-localisation. By fitting these data with the weak anti-localisation theory [6], we estimated the phase relaxation and spin-orbit coupling lengths. The phase relaxation length was found to be 480 nm at 500 mK and to be reduced to 410 nm with increasing temperature up to 5 K as expected. These values are two orders of magnitude smaller than previously reported value (12 μm) in a 60-nm-thick Au film measured at 300 mK [7]. Such reduction may be induced by scattering at the Cr/Ag interfaces. The spin-orbit coupling length, on the other hand, was found to be 240 nm at 500 mK almost independent of temperature.

In summary, we have successfully fabricated a quantum device consisting of a ferromagnetic nanopillar enclosed by a non-magnetic nanoring. As the first step towards the demonstration of a spin-polarised persistent current, we observed AB oscillation and weak anti-localisation in the nanoring below 5 K. Unfortunately we could not measure the AB oscillation induced by the Berry phase. We will improve our devices by (i) removing the Cr seed layer in the nanoring, (ii) replacing Au with Ag to increase the spin diffusion length, (iii) narrowing the width of the nanoring and (iv) minimising the nanofabrication damage onto the nanopillar.

References

[1] D. Loss and P. M. Goldbart, *Phys. Rev. B* **45**, 13544 (1992).
[2] Y. Imry, *Introduction to Mesoscopic Physics* (Oxford University Press, Oxford, 1977).
[3] L. Vila *et al.*, *Phys. Rev. Lett.* **98**, 027204 (2007).
[4] K. Sekiguchi *et al.*, *Phys. Rev. B* **77**, 140401(R) (2008).
[5] A. Hirohata *et al.*, Experimental demonstration of a persistent current in a Au ring under the presence of a non-uniform magnetic field, *4th Int'l. Workshop Spin Curr.* (9 Feb. 2010, Sendai, Japan)
[6] E. Akkermans and G. Montambaux, *Mesoscopic Physics with Electrons and Photons* (Cambridge Univ. Press, Cambridge, 2007).
[7] V. Chandrasekhar *et al.*, *Phys. Rev. Lett.* **67**, 3578 (1991).
[8] S. Norimoto, K. Tanabe, M. Ferrier, T. Arakawa, K. Kobayashi, A. Hirohata, M. Mizuguchi, K. Takanashi, Transport measurement on a single Aharonov-Bohm ring in the presence of an inhomogeneous magnetic field, *Phys. Soc. Jpn. Autumn Meeting* (to be presented on Sep. 2014, Kasugai, Japan).

Keywords: spin current, Aharonov-Bohm effect, nanowire
Atsufumi Hirohata (University of York)
E-mail: atsufumi.hirohata@york.ac.uk
http://www~users.york.ac.uk/~ah566/

Skew scattering, spin Hall effects and muons in spintronics

Abstract: Calculations were made directed to the understanding and control of skew scattering mechanisms for electrons in solids. This is crucial in the search for suitable compounds for the efficient conversion of charge and spin currents to enable future spintronic devices. Theory was developed to understand the magnitude of spin Hall angles measured recently in metallic alloys. In parallel calculations were made to explain the sensitivity of muon spin relaxation to non-equilibrium states of doped semiconductors.

While at the IMR, in the Nojiri laboratory, I continued research directed towards the quantitative understanding of skew scattering phenomena that determine anomalous transport coefficients in the Anomalous and Spin Hall Effects. In the the sign of the spin Hall angle (SHA), i.e. the direction of the induced transverse current was often ignored. This was partly because the primary concern was the small magnitude of the Hall angle, and the search for larger values. As measurements become more systematic, the issue of the sign has became more central; in particular following the report of a very large spin Hall angle of -0.24 at low temperatures in a CuBi alloy. . This result contrasted with previous predictions of a very large Spin Hall Angle, but of opposite sign for Cu doped with Bi impurities. From this discrepancy, it had been claimed in the literature that this could be attributed to none of the conventionally known skew-scattering , side-jump nor intrinsic mechanisms. This would seem to be a serious challenge to our understanding of the Spin and Anomalous Hall effects. By re-examining this issue we showed that in fact a phase shift analysis with the p-orbitals and consistent definitions with quoted experimental results removes any contradiction to a skew scattering mechanism, and thus we restore the possibility of properly microscopic understanding of the effects. There remains a possibly significant difference in the magnitude of the angle and we advanced an explanation[1], backed up with calculation of local electronic structure which showed a significant enhacement by Bi atoms at the Cu surface. This effect of the localization of the impurity state on the surface as shown in Fig 1:

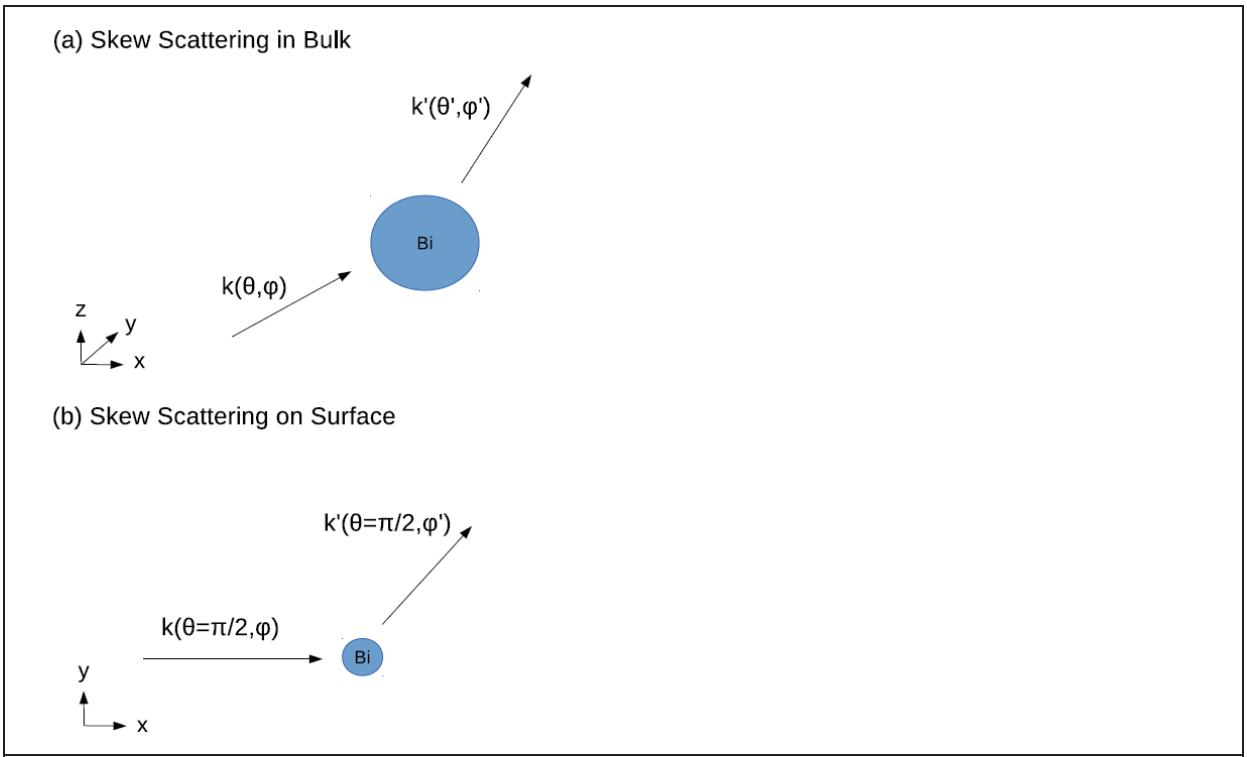

Fig.1 shows schematically the enhanced scattering of Bi impurities on the surface of Cu

hybridization between impurity and surface is shar ply decreased, which factor, combined with the effects of Coulomb correlations enhanced skew scattering.

Recently a small positive spin Hall angle of a few percent, was observed experimentally in nonmagnetic CuIr alloys and attributed predominantly to an extrinsic skew scattering mechanism, which in this case really is opposite in sign to calculations from an extrinsic skew scattering. We therefore reonsidered the SHA in CuIr alloys, with full inclusion of effects of the local electron correlation in 5d orbitals of Ir impurities beyond local density functional methods. In this case the negative angle calculated ignoring such local electron correlation, becomes positive once the correlation U approaches a realistic value. The mechanism can be understood qualitatively as being caused by the redistribution of charge in the local extended impurity state of d symmetry into less correlated s and p extended impurity orbitals. As skew scattering, an interference effect between diffffferent scattering channels, is sensitive to shifts in weight this is sufficient to switch the sense of skew scattering from being predominantly in one direction to another. One might then speculate on future ways to control the sign of spin currents by manipulating the occupation number of impurities.

2

In parallel with this activity we have provided a theoretical explanation for laser-pumped experiments on muon precession performed at J-Parc , that have established that muonium can be a tool in spintronics for following non-equilibrium spin polarizations of the conduction electrons. In n-type GaAs, a puzzling result was that even for the charge state of negatively charge Muonium-, which is the atomic-like state

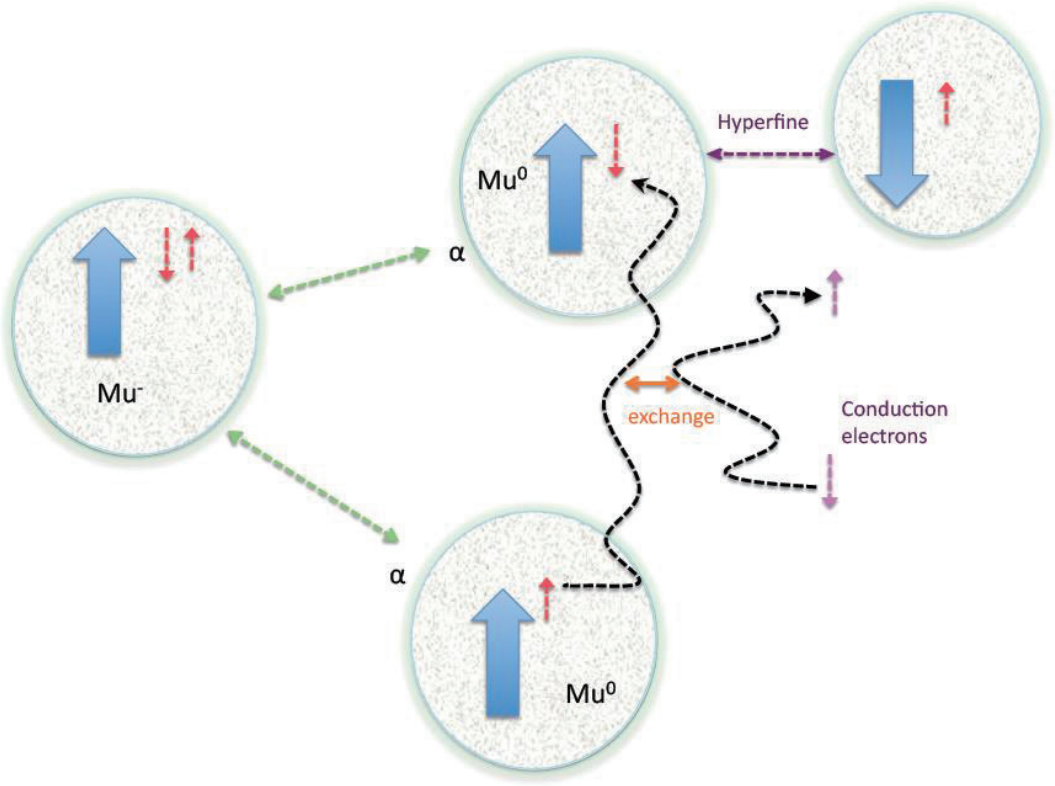

Fig. 2 Schematic theory of muon spin relaxation in negatively charged muonium.

of a positive muon and two bound electrons, there was apparent exchange with conduction electron spins. This is more problematic than previously seen exchange of spin in neutral muonium, as it is difficult to see how spin exchange can occur significantly in what is an spin singlet state of the two electrons. Estimates for the vacuum bound state of muonium give too weak an effect to be relevant to the experiments. We have proposed[2] a mechanism to explain the sensitivity of negatively charged Muonium ions to the spin-polarization of semiconductors in terms of the coherent mixing of charge states induced by hybridization with the semiconducting host. This is shown schematically in Figure 2.

3

Estimations of the parameters in a model Hamiltonian for different semiconducting hosts allow comparison to scattering times for Silicon and n-type GaAs and the predicted dependence on temperature and doping should lead in the future to tests of the theory..

Keywords: spintronic, magnetic properties, nanowire,

Timothy Ziman ziman@ill.fr

References

[1] B. Gu,, Zhuo Xu, M. Mori, T. Ziman, S. Maekawa,, Sign and Magnitude of Spin Hall Effect in CuBi Alloys submitted (2014) arXiv:1402.3012
[2] B. Gu, M. Mori, T. Ziman, S. Maekawa,, Negatively Charged Muonium as a Detector of Electron Spin Polarization: a Puzzle and a Possible Theory",Jap. Phys. Soc. Conf. Proc. 2 010301 (2014)
[3]Z. Xu, B. Gu, M. Mori, T. Ziman, S. Maekawa,, "Sign change of the spin Hall effect due to electron correlation in nonmagnetic CuIr alloys", submitted to Phys. Rev. (2014) arXiv 1405.7449

Comments:	4 pages, 2 figures
Subjects:	Materials Science (cond-mat.mtrl-sci)
Cite as:	arXiv:1402.3012 [cond-mat.mtrl-sci]

Classical spin dynamics simulations of the magnetic properties of a one-dimensional carboxylate-bridged Mn(III) Salen complex

We investigated the magnetic properties of the one-dimensional carboxylate-bridged Mn(III) Salen complex [Mn(5-Br-salen)(Br-Acetate)]$_n$ by means of classical Monte Carlo simulations. Based on a simple nearest-neighbor Heisenberg model with uni-axial anisotropy we found that the system's magnetic structure is that of a non-collinear canted antiferromagnetic spin chain.

The synthesis of new magnets, i.e. magnetic materials that retain their magnetization in the absence of a magnetic field, is a major challenge for future storage applications on the nano scale. Single-chain magnets (SCM) are composed of magnetically isolated chains that can be individually magnetized. As purely one-dimensional systems are known to have a long-range order only at T = 0 K, these SCM materials remains in their paramagnetic state at any finite temperature. Nevertheless, the combination of a large uni-axial anisotropy and large magnetic interactions between the high-spin magnetic units of the chain promotes long relaxation times and the system can behave as a magnet.

Recently, the one-dimensional carboxylate-bridged Mn(III) salen complexes [Mn(5-Br-salen)(Br-Acetate)]$_n$ (Fig. 1) has been synthezised and first experimental results suggest that this system can be understood as a canted antiferromagnetic SCM [1].

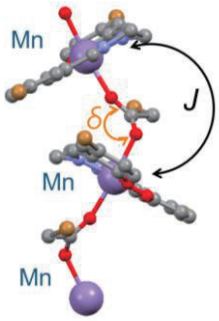

Fig.1 Magnetic model of the one-dimensional chain magnet [Mn(5-Br-salen)(Br-Acetate)]$_n$

Since each Mn(III) ion has quite a large spin quantum number of s = 2 we have simulated the system by taking into account a classical Heisenberg model with a single exchange interaction J between nearest neighbor Mn ions as well as a uni-axial anisotropy D. The anisotropy axes form a planar zig-zag pattern with an inner angle δ (Fig. 1). Since the measurements were based on powder samples we have performed Monte Carlo simulations with multiple magnetic field directions and subsequent averaging. In order to avoid boundary effects, i.e. to simulate an infinite chain, we had to use 80 spins. By fitting to the experimental susceptibility data we found excellent agreement for the high temperature regime using the parameters J/k_B = -2.17 K and D/k_B = -3.17 K as well as a g-value of g=1.97. These results are consistent with the assumption of a non-collinear canted antiferromagnetic spin structure. At temperatures below 20 K we found a deviation of our model to the experimental data (Fig. 2). By taking into account dipole-dipole interaction within a chain and between neighboring chains we get a better agreement, however still not a match. Further effects are currently under investigation.

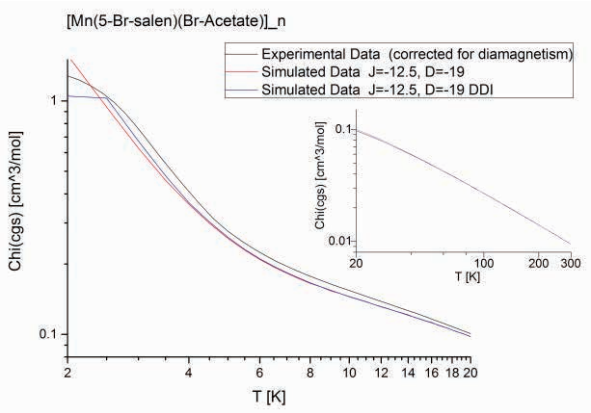

Fig. 2 Comparison of experimental and simulated susceptibility data

References

[1] Y. Aono, K. Kagesawa, K. Katoh, B. K. Breedlove, M. Yamashita, 4th Asian Conference on Coordination Chemistry, Korea (2013).

Keywords: magnetic, magnetic properties, simulation
Christian Schröder (Bielefeld University of Applied Sciences)
E-mail: christian.schroeder@fh-bielefeld.de
http://www.fh-bielefeld.de/fb3/schroeder

Development of growth technology for large size bulk and shaped growth on scintillator, piezoelectric and halogen single crystals

Within my stay at ICC-IMR as invited professor during 1 month few new crystals for scintillator and piezoelectric applications were grown at a first time by the Czochralski technique. The application of such crystals can help with the development of new generation of high sensitive X-ray identification devices and for new generation of combustion sensor for car engines with the aim of efficiency increase of combustion rate (and the reduction of emission amount).

The main reason of my invitation was the further development of bulk crystal growth technique. At last 10-15 years a lot of interesting discoveries in the field of crystals were made in the area related to miniaturization of films and fibers up to nano size. As a result a lot of crystal growth researchers changed their activity direction in accordance with this modern tendency. Unfortunately a lot of expertise related to bulk crystal growth was simply lost in the world at that time. However, the need of industry in the big variety of high quality and big size bulk crystals has been increasing. And I was very glad to accept the invitation of ICC-IMR for work during 1 month as invited professor in the area related exactly to development of crystal growth technology of big bulk crystals.

My main attention during stay at IMR was focused on 2 big groups of bulk crystals – for scintillatior applications and for piezoelectric applications. Both of these groups of crystal are very important for Japan now. I worked for the development of bulk crystal growth technology by the Czochralski technique during many years [1-2] and I expected that my experience would be useful for joint research work at ICC-IMR.

The Scintillator crystals for the application in new generation of dosimeters became extremely important after 2011 great earthquake in Japan and followed incident at Fukushima nuclear power plant. In the IMR laboratory of professor Yoshikawa the very promising material for such application – Ce-doped Gd-Al-Ga garnet single crystal was developed before [3]. During my stay in IMR I was happy to join the experiments for the improvement of crystal growth technology with the final aim of growth of such crystals with the size up to 2-3 inch in diameter and stable set of parameters acceptable for the application in the new generation of X-ray high sensitive devices.

The second big group of bulk crystals (piezoelectric) also became a very hot topic now. At present all highly developed countries in the world are involved into vast actions for the decrease of air pollutions caused by cars emission. Recently it was found that the direct sensing of the torque oscillation in the engine section by use of the combustion sensor in comparison with traditional oxygen sensors can improve efficiency of combustion rate (and the reduction of emission amount) up to 10 %. However the wide application of such systems is limited by the lack of crystals which can work in combustion sensors at very high temperature. Recently, 2 new piezoelectric crystals were suggested for this application –$Ca_3TaGa_3Si_2O_{14}$ and $Ca_3NbGa_3Si_2O_{14}$. These 2 crystals can work as sensors up to 1400 C. During my stay at IMR jointly with the researchers and students of Yoshikawa laboratory we paid a big attention to the development of stable growth technology of these two crystals. One of the results of our joint experiments ($Ca_3NbGa_3Si_2O_{14}$ crystal) is shown

on Fig. 1 In opposite with known reports [4-5] this crystal was grown in Air atmosphere using Pt crucible (usually researchers tried to use of Ar atmosphere and Ir crucibles) .Such conditions can simplify such crystals production in future. Also, I investigated the possibility to substitute some amount of Ga ions in $Ca_3TaGa_3Si_2O_{14}$ crystal by Al ions for further improvement of piezoelectric properties and decreasing of

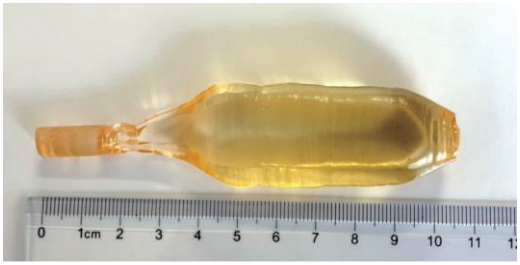

Fig. 1 As-grown $Ca_3NbGa_3Si_2O_{14}$ crystal

production cost. The most successful result of these experiments is shown on Fig. 2 It is expected that the piezoelectric properties of this crystal ($Ca_3Ta(Al_{0.2}Ga_{0.8})_3Si_2O_{14}$) will be higher than for usual one. It was confirmed that it is possible to produce this crystal by the conventional Czochralski technique with the size and quality acceptable for the future commercial application.

Of cause, during so short time (1 month) a lot of our joint ideas were not realized. However,

Fig.2 as-grown $Ca_3Ta(Al_{0.2}Ga_{0.8})_3Si_2O_{14}$ crystal

I am sure that we will continue the fruitful scientific cooperation with my colleagues at IMR for the successful development of important and interesting research which we have started.

References

[1] T. Fukuda, K. Shimamura, V.Kochurikhin, V. I. Chani, B. M. Epelbaum, S. L. Baldochi, H. Takeda, A. Yoshikawa, J. Mat. Sci.: Materials in Electronics 10 (1999) 571-580

[2] A. Yoshikawa, M. Nikl, H. Ogino, J.B. Shim, V.V. Kochurikhin, N. Solovieva, T. Fukuda Nuclear Instruments and Methods in Physics Research A 537 (2005) 76–80

[3] Kei Kamada, Takayuki Yanagida, TakanoriEndo, KousukeTsutumi, YoshiyukiUsuki, Martin Nikl, YutakaFujimoto, AkihiroFukabori, AkiraYoshikawa Journal of Crystal Growth 352 (2012) 88–90

[4] Zengmei Wang et al., Journal of Crystal Growth 253 (2003) 378–382

[5] Hiromitsu Kimura, Satoshi Uda, Oleg Buzanov, Xinming Huang, Shinji Koh J Electroceram 20 (2008) 73–80

Keywords: Crystal growth, piezoelectric, Scintillator

Full name: Vladimir Kochurikhin, General Physics Institute, Moscow, Russia
E-mail: kochurikhin@mail.ru
http://www.gpi.ru

Large plastic deformation of interstitial oxygen added Ti-Nb-Ta-Zr alloys for biomedical applications

Plastic deformation behavior was investigated among Ti-29N-13Ta-4.6Zr alloys (TNTZ) with oxygen content of 0.1−0.7 mass%. With the increase in oxygen content, the tensile strength and 0.2% proof stress of all the alloys increase normally, while their elongations reveal special change, which is contradictory to that reported conventionally. The elongation firstly decreases as usual, but then increases with the increase in the oxygen content. Therefore, TNTZ with high strength and high ductility due to the addition of high oxygen content (0.7mass%) can be obtained.

An attractive β-type titanium alloy, Ti-29Nb-13Ta-4.6Zr alloy (TNTZ), which is composed of non-toxic and allergy-free elements, has been developed for biomedical applications. TNTZ exhibits low Young's modulus of around 60GPa, which is relatively similar to that of bone (10-30 GPa). However, it should be noted that its strength is still not sufficiently high to satisfy the requirements of a long service life. It is, therefore, necessary to further increase the strength and not to increase concomitantly the Young's modulus. From this viewpoint, interstitial elements are very promising because their addition to TNTZ is expected to improve its strength via solution strengthening. Therefore, the effect of oxygen content, particularly at the rather high level, on the tensile properties of TNTZ was investigated in this study [1,2].

In this study, three types of TNTZ ingots containing 0.14 mass%, 0.33mass%, and 0.70mass% oxygen were prepared. They were hot rolled at 1273K, followed by air cooling (HR14, HR33, and HR70, respectively). Then, the hot rolled specimens were subjected to solution treatment at β transus temperature + 50 K for 3.6 ks, followed by water quenching (HRST14, HRST33, and HRST70, respectively).

The microstructures of HR14, HR33, HR70, HRST14, HRST33, and HRST70 were observed by optical microscopy (OM). In all the cases, the microstructures consisted of a single phase, and the grain size and its morphology of HRST series were more uniform as compared to those of HR series. The occurrence of some small grains in the microstructures of HR series indicates the emergence of recrystallization during hot rolling. The single phase shown in every specimen was identified as β phase by X-ray diffraction (XRD).

Figure 1 shows the Young's moduli of HR14, HR33, HR70, HRST14, HRST33, and HRST70. As a reference, the Young's modulus of Ti-6Al-4V ELI alloy, that is a conventional titanium alloy for use in biomedical applications is also shown in this figure. The Young's moduli of both HR and HRST series increase with increasing oxygen content. The Young's moduli of HR70 and HRST70 are a little higher than that of usual TNTZ, but less than around 75 GPa, which is much less than

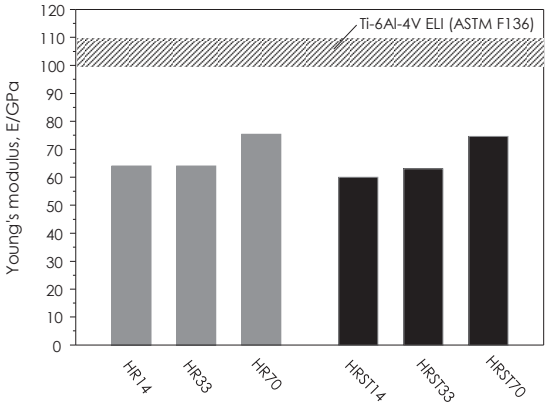

Fig.1 Young's moduli of TNTZ containing 0.14mass%, 0.33mass%, and 0.70mass% oxygen subjected to hot rolling (HR14, HR33, and HR70), and subsequent solution treatment (HRST14, HRST33, and HRST70).

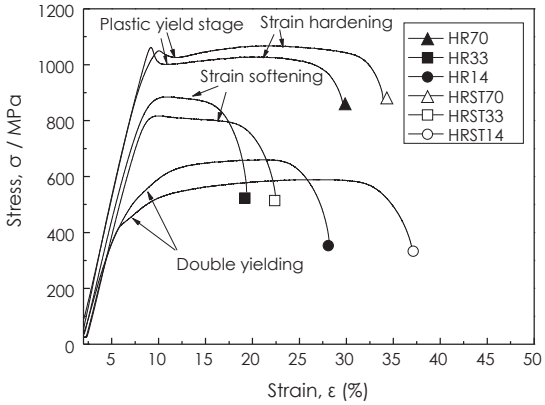

Fig.2 Tensile stress-strain curves of TNTZ containing 0.14mass%, 0.33mass%, and 0.70mass% oxygen subjected to hot rolling (HR14, HR33, and HR70), and subsequent solution treatment (HRST14, HRST33, and HRST70).

that of Ti-6Al-4V ELI. According to the microstructural analysis using OM and XRD, every specimen consisted of the single β phase. Therefore, it is considered that the increase in Young's modulus of both HR and HRST series could be attributed to oxygen dissolution in the β phase.

Figure 2 shows the tensile stress-strain curves of HR14, HR33, HR70, HRST14, HRST33, and HRST70. With the increase in oxygen content, the tensile strength increases, but the elongation firstly decreases and then increases in both HR and HRST series. This result is contradictory to that reported conventionally. The previous study indicates that the tensile strength increases with the addition of oxygen, but the elongation correspondingly decreases [3]. In this study, HR70 and HRST70 exhibit particularly good ductility in spite of high strength. Both the tensile strength and elongation of HR70 and HRST70 are larger than those of Ti-6Al-4V ELI (minimum tensile strength: 860MPa, minimum elongation: 10%, which are registered values in the ASTM F136 standard).

Further, during the tensile tests, a double yielding occurs in HR14 and HRST14, which is well-known phenomenon for the deformation-induced martensite transformation. The occurrence of the deformation-induced martensite improves the elongation and enhances the slight strain hardening. After tensile tests, in HR14 and HRST14, deformation-induced α'' martensite laths were clearly observed by OM as shown in Fig. 3, and these laths were not present in the undeformed state (before tensile test). The α'' phase could be correspondingly detected by XRD and transmission electron microscopy (TEM). Furthermore, a plenty of dislocations could be observed in deformation-induced α'' phase by TEM. However, no new phase could be observed and detected in HR33, HR70, HRST33, and HRST70 after tensile tests. This result indicates that the addition of oxygen decreases the martensite transformation start temperature (Ms), leading to the suppression of α'' phase formation.

Moreover, the tensile stress-strain curves of HR70 and HRST70 reveal obvious yielding and strain hardening. Strain hardening suggests the possibility of plastic deformation mechanism being under the aid of dislocation motion. However, the mechanism for large elongation of these specimens is still unclear. This point will be investigated by collaboration with Professor Niinomi's group in future.

References

[1] F. Geng, M. Niinomi and M. Nakai, Mater. Sci. Eng. A 528, 5435-5445 (2011).
[2] C.J. Boehlert, H.H. Liu, M. Niinomi, M. Nakai, J. Hieda and K. Cho, International Conference on Martensitic Transformations 2014 (ICOMAT-2014), Bilbao, Spain, Jul. 6-11, 2014.
[3] M. Nakai, M. Niinomi, T. Akahori, H. Tsutsumi and M. Ogawa, Mater. Trans. 50, 2716-2720 (2009).

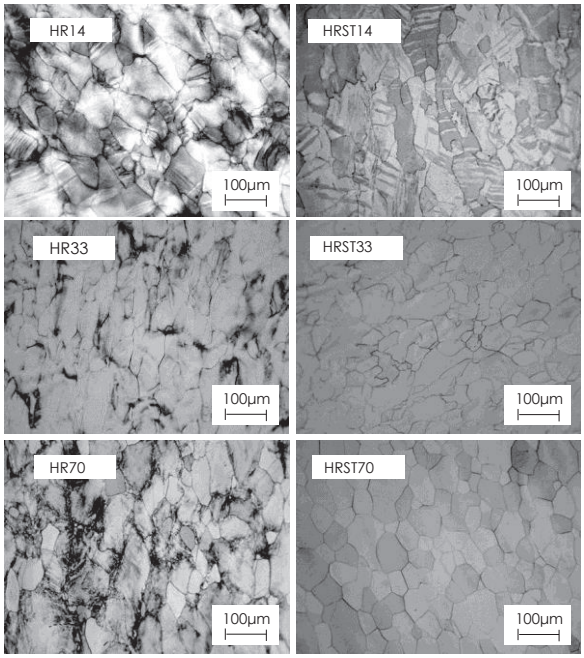

Fig.3 Optical micrographs of TNTZ containing 0.14mass%, 0.33mass%, and 0.70mass% oxygen subjected to hot rolling (HR14, HR33, and HR70) and subsequent solution treatment (HRST14, HRST33, and HRST70) after tensile tests. The observation was carried out after polishing.

Keywords: metal, deformation, Young's modulus
Carl J. Boehlert (Michigan State University)
E-mail: boehlert@egr.msu.edu
http://www.egr.msu.edu/~boehlert/GROUP

Activity Report

Workshops

FY 2013 Workshops

No.	Chairperson	Title of Workshop	Place	Date
13WS1	T. Goto	The 8th International Workshop on Biomaterials in Biosis-Abiosis Intelligent Interface Science	Zao, Miyagi	2013.8.29-8.30
13WS2	M. Fujita	Superconductivity Research Advanced by New materials and spectroscopies	IMR Lecture Hall	2013.7.23-7.25
13WS3	A. Makino	6th International Workshop on Amorphous and Nanostructured Magnetic Materials - ANMM'2013	TRUST CITY Conference, Sendai	2013.10.1-10.3

The 8th International Workshop on Biomaterials in Biosis-Abiosis Intelligent Interface Science

- Innovative Research for Biosis-Abiosis Intelligent Interface Summer Seminar 2013 -

Developments of biomaterials have recently become a crucial issue because of strong demands for replacing various parts in human-body with artificial products. The experts, researchers and students from different fields related to biomaterials gathered at the 8th International Workshop on Biomaterials in Biosis-Abiosis Intelligent Interface Science 2013 on Aug. 29th–30th at Sendai, Japan. The invited lectures by 6 experts from abroad and 22 papers provided valuable opportunity for cross-over discussion, interdisciplinary idea sharing and new collaboration to develop and establish the intelligent interface science on biomaterials.

Interdisciplinary and international activities are necessary to develop the biomaterials, such as artificial bone and tooth, because the biomaterials should meet the various demands to control biofunctionalities and mechanical properties in a wide range from nano- to micro-scale, as well as compatibility with human body. Three Institute in Tohoku University, namely Institute for Materials Research (IMR), Graduate School of Dentistry and Graduate School of Biomedical Engineering, have been collaborating and involved the 5-year project on Biomaterials in Biosis-Abiosis Intelligent Interface Science. As the series of international forums in the frame this project, the 8th International Workshop on Biomaterials in Biosis-Abiosis Intelligent Interface Science 2013 in conjunction with Innovative Research for Biosis-Abiosis Intelligent Interface Summer Seminar 2013 was held on Aug. 29th–30th, 2013, at Miyagi Zao, Sendai.

The 2-days technical program in this workshop included 28 papers in which 6 invited lectures were given by experts on biomaterials from Korea, China and Australia. About 62 participants of professors, researchers and students attended in the workshop.

Prof. Qing Li provided a lecture on soft tissue driven bone remodelling. The lecture by Prof. Jeong-Tae Koh was on roles of orphan nuclear receptor COUP-TFII in osteoblast differentiation. The state-of-the-art research on surface modifications of biomaterials was provided by Prof. Yongsheng Zhou, entitled "the effects of novel surface modifications on bone regeneration", and by Prof. Young-Jun Lim, entitled "Ultraviolet-light induced photocatalytic bactericidal effects on modified titanium surfaces". Prof. Xing-quan Jiang gave a lecture on Tissue engineering and regeneration medicine for bone deficiency and dental implantation, while the lecture by Prof. Bangcheng Yang was on Ti metals with bioactivity and antibacterial properties. In addition to the invited lectures, presentations by speakers with various academic backgrouds provided valuable opportunity for sharing updated and interdisciplinary viewpoints and ideas to the all participants. The collaborative discussion had great contributions to the development on the intelligent interface science on biomaterials.

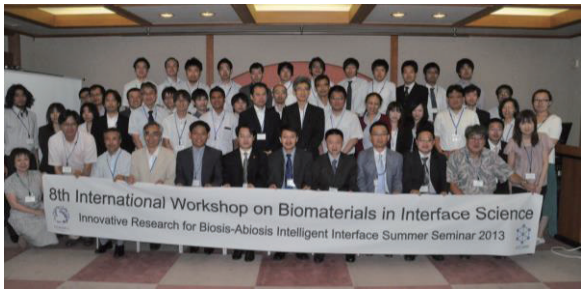

Fig. 1 A group photo at 8th International Workshop on Biomaterials in Interface Science (Innovative Research for Biosis-Abiosis Intelligent Interface Summer Seminar 2013) at the conference hall, Miyagi Zao, Sendai.

Fig. 2 One shot in an invited lecture. Participants from various fields, such as dentistry, medical science and material engineering, eagerly listen to the lecture.

Keywords: biomedical, ceramic, metal
Takashi GOTO (Multi-Functional Materials Science)
E-mail: goto@imr.tohoku.ac.jp
http://interface.imr.tohoku.ac.jp/

Superconductivity research advanced by new materials and spectroscopies

In this workshop, novel physics brought through new materials and the quantum beams at large facility were intensively discussed. Many progresses in the research of unconventional superconductivity and their related phenomena emerging from the charge, spin and orbital degrees of freedom were reported. The strategic and educational use of quantum beam facility such as J-PARC and Spring-8 for the research of material science was also addressed.

The international workshop "Superconductivity research advanced by new materials and spectroscopies" was held on July 23rd-25th, 2013 in the lecture Hall of Institute for Materials Research, Tohoku University. This workshop aimed to discuss recent experimental and theoretical development in the research of unconventional superconductivity

Searching for high-Tc superconducting materials and understanding the electronic states are exciting and challenging field in physics of strongly correlated electron system as well as materials science. On the other hand, various spectroscopy techniques with quantum beams such as neutron, muon and synchrotron X-ray, are indispensable for the study of dynamical properties of charge, spin and orbital degrees of freedom. Therefore, the discussion about new researches on novel physics potentially brought through new materials and the world highest intensity quantum beams are quite important. We selected following topics as the main target and exchanged ideas.

1: High-Tc superconductivity in cuprate oxides and related phenomena
2: Superconductivity in Fe-based compound and the mechanism
3: New superconducting materials and exotic phenomena

The advanced spectroscopic technique and its strategic use were also discussed. This workshop provided a unique opportunity to discuss and exchange the finding and ideas on recent and long-standing researches. The young scientists interacted with senior researches through various informal discussions. We would like to thank all participants and the support from ICC-IMR for the success of the workshop.

Fig. 1 A picture of workshop. More than 100 researchers including many young scientists participated in the workshop.

Keywords: high-tc iron-based pnictide superconductivity, electronic material, neutron scattering
Masaki Fujita (Material Processing and Characterization Division)
E-mail: fujita@imr.tohoku.ac.jp
http://www.qblab.imr.ac.jp/ index.html

Activity Report

KINKEN WAKATE

FY 2013 KINKEN WAKATE

No.	Chairperson	Title of Workshop	Place	Date
13Wakate	K. Fujiwara	10th Materials Science School for Young Scientists (KINKEN-WAKATE 2013)	TRUST CITY CONFERENCE	2013.11.21-22

KINKEN-WAKATE 2013 -10th Materials Science School for Young Scientists-

KINKEN-WAKATE 2013 was held on November 21st-22nd, 2013, at TRUST CITY CONFERENCE, SENDAI. The aim of KINKEN-WAKATE 2013 was to provide comprehensive lectures of crystal growth and to promote exchange of ideas and collaborations among young scientists. Participants deepened understanding of crystal growth through lectures by four leading researchers and actively discussed each other through poster presentations by young scientists.

KINKEN-WAKATE 2013 was comprised of the lecture session and the poster session. The program began with the greetings of Prof. Niinomi who was the director of IMR on the morning on Nov. 21st (Fig. 1). Subsequently, the lecture session was carried out as follows.

Nov. 21st
Lecture 1: Epitaxial growth (1)
Lecture 2: Epitaxial growth (2)
by Prof. Tatau Nishinaga (Professor emeritus at the University of Tokyo).

Lecture 3: Bulk crystal growth (1)
Lecture 4: Bulk crystal growth (2)
by Prof. Peter Rudolph (Crystal Technology Consulting (CTC)).

We learned fundamentals of 2D nucleation, surface morphology, surface diffusion, etc., and technologies of thin film growth, such as MBE, MOCVD, and Micro-channel epitaxy(MCE), in Lectures 1 and 2. Thermodynamics, kinetics, and transports of heat and mass during melt growth processes were lectured in Lecture 3, and growth technologies of variety of bulk crystals were explained in Lecture 4.

Nov. 22nd
Lecture 5: Fundamental crystal growth mechanisms
Lecture 6: Surface melting: hot low-temperature science
by Prof. Gen Sazaki (Hokkaido University).

Lecture 7: Defect Engineering (1)
Lecture 8: Defect Engineering (2)
by Prof. Thomas Kuech (University of Wisconsin-Madison).

We could understand step growth mechanisms on a protein crystal surface and also understood the formation of quasi-liquid layers on an ice crystal surface in Lectures 5 and 6. Thermodynamics, electrical properties, and engineering of point defects were explained in detail in Lectures 7 and 8.

Through those 8 splendid lectures, our understanding for crystal growth deepened.

In the poster session, young scientists gave 3 min oral short presentations in English (Fig. 2) and poster presentations.

KINKEN-WAKATE 2013 finished a success with a convivial party on the evening on 22nd.

Fig. 1 The four lecturers were introduced in the opening talk by Prof. Niinomi.

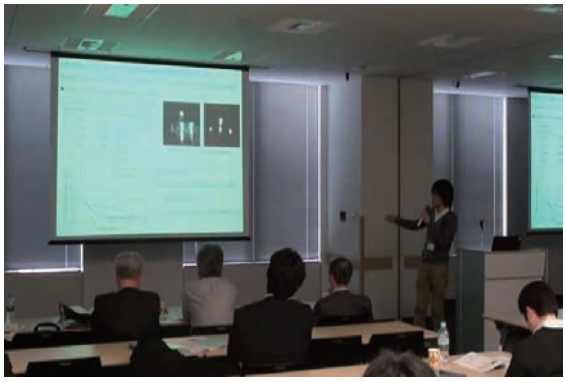

Fig. 2 Short presentations by young scientists

Keywords: crystal growth, defects
Kozo Fujiwara (Crystal Chemistry Division) and Masaki Mizuguchi (Magnetic Materials Division)
E-mail: kozo@imr.tohoku.ac.jp, mizuguchi@imr.tohoku.ac.jp
http://www.imr.tohoku.ac.jp/ja/info/event-report/2013/1121.html

Activity Report

Short-term Visiting Researchers

FY 2013 Short-term Visiting Researchers

Application No.	Name	Host	Proposed Research	Title	Affiliation	Term
13SV1	Xiaoli Zhao	M. Niinomi	Development of Zr-Nb Alloys with Changeable Young's Modulus for Spinal Fxation Applications	Assistant Professor	Northeastern University, China	2013.9.1-11.27
13SV2	Hong Wu	A. Chiba	Microstructure and Tribological Behavior of Ni-free Ti-Based Bulk Metallic Glasses for Biomedical Applications	Assoc. Professor	Central South University, China	2013. 12.7-12.24
13SV3	Takuya Yamamoto	K. Nagai	Advanced Microstructural Characterization of New Radiation Induced Defects in RPV Steels	Research Engineer	University of California Santa Barbara, USA	2013. 7. 17-8. 3
13SV4	Hyung-Seop Shin	S. Awaji	Electro-Mechanical Property Evaluation in HTS CC Tapes Under Magnetic Field	Professor	Andong National University, Korea	2014. 2. 3-2. 9
13SV5	Junichiro Kono	H. Nojiri	Development of a Compact Pulsed Magnet for High-Field Magneto-Optical Studies of Carrier and Exciton Dynamics in Nanostructures	Professor	Rice University, USA	2014. 3.5-3.16 Dr. Theo Fischer, Ruhr-University Bochum, Germany

Beta-type Zr-Nb alloys with changeable Young's modulus for spinal fixation applications

Beta type Zr-Nb alloys with changeable Young's moduli are developed for spinal fixation applications. Before deformation, the alloys exhibit low Young's modulus to keep the mechanical compatibility. After deformation, the Young's moduli of all the alloys increase with different range. The increase in Zr-15Nb and Zr-17Nb reach 34.3% and 26.5%, respectively. The EBSD and TEM results indicate the significant increase in the Young's modulus of these two alloys is attributed to the deformation-induced ω phase.

For spinal fixation applications, the alloys with changeable Young's modulus are preferred to meet the demands of both surgeons and patients. The alloys should possess a low Young's modulus before deformation to keep the mechanical compatibility, and a high Young's modulus at the deformed part with the deformation during surgery to lower the springback [1].

Each Zr-*x*Nb (*x* = 13, 15, 17, 19, 21, 23 mass%) (200g) were prepared by levitation melting. The ingots were then homogenized at 1373K for 21.6 ks and hot-forged at 1273K (both processes were performed in an argon atmosphere), after which they were quenched in ice water and the air-cooled, respectively. Then the hot rolled plates were solution treated in vacuum at 1123 K for 3.6 ks and quenched in ice-water. Some of the solutionized plates were cold rolled with a reduction ratio of around 10% at room temperature. As the final treatment, the solution treatment and cold rolling were labeled as ST and CR, respectively.

After solution treatment, each of the Zr-xNb (x = 13, 15, 17, 19, 21, 23 mass%) alloys consists of equiaxed β phase and tiny dispersive ω phase, which were observed by TEM. The intensity of the athermal ω phase decreases with increase in the Nb content. In addition, in the Zr-xNb (x = 13, 15, 17 mass%) alloys, some unknown phase with acicular structure is visible. These phases disappear with increase in the Nb content.

Figure 1 shows the Young's moduli variation of each alloys subjected to solution treatment and cold rolling. All the novel designed alloys exhibits low Young's moduli of <70 GPa; this value is much lower than those of SUS 316L stainless steel (SUS 316L), commercially pure titanium (CP Ti), and Ti-6Al-4V ELI alloy (Ti64 ELI) [2], which are currently widely used for spinal fixation applications. The Young's moduli of Zr-15Nb and Zr-17Nb are lower than 60GPa ; this value is much closer to that of human bones compared with the previous developed Ti-30Zr-Cr-Mo [3], Ti-Cr [4], Ti-Mo [5], and TNTZ-Cr [6] alloy. Therefore, the Zr-Nb alloy exhibits excellent mechanical compatibility. After cold rolling, the Young's moduli of all the alloys increase compared with those under ST conditions. The increase in Zr-15Nb and Zr-17Nb reach 34.3% and 26.5%, respectively. The EBSD and TEM results indicate that deformation-induced ω phase exists in both Zr-15Nb and Zr-17Nb alloy, however, the deformation-induced ω phase in Zr-15Nb is accompanied with the deformation-induced {332}<113> mechanical twin, while the deformation-induced twin is not visible in Zr-17Nb alloys. The significant increase in the Young's modulus is attributed to the deformation-induced ω phase.

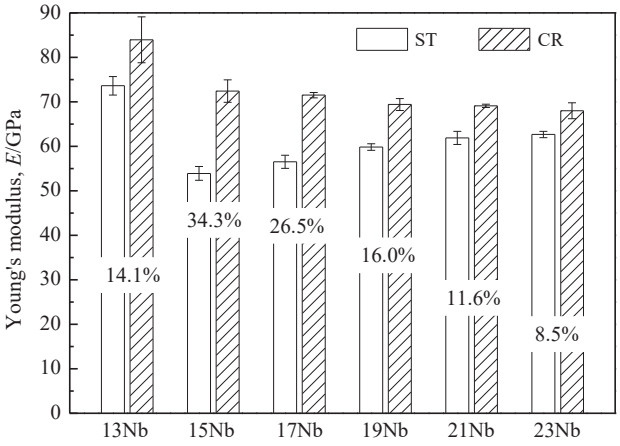

Fig. 1 Young's moduli of Zr-Nb alloys subjected to solution treatment (ST) and cold rolling (CR).

References

[1] M. Nakai, M. Niinomi, X. F. Zhao, X. L. Zhao, Materials Letters, 65(4), 688-690 (2011)
[2] X.L. Zhao, M. Niinomi, M. Nakai, T. Ishimoto and T. Nakano, Mater. Sci. Eng. C, 31, 1436 -1444 (2011).
[3] X. Zhao, M. Niinomi, M. Nakai, G. Miyamoto, and T. Furuhara, Acta Biomater. 7(8), 3230-3236 (2011)
[4] X.F. Zhao, M. Niinomi, M. Nakai, J. Hieda, T. Ishimoto, and T. Nakano, Acta Biomater. 8(6), 2392-2400 (2012)
[5] X.F. Zhao, M. Niinomi, M. Nakai, and J. Hieda, Acta Biomater. 8(5), 1990-1997 (2012)
[6] Q. Li, M. Niinomi, J. Hieda, M. Nakai, and K. Cho, Acta Biomater. 9(8), 8027-8035 (2013)

Keywords: Young's modulus, biomedical, microstructure
Xiaoli Zhao (Materials institute, Schools of Materials and Metallurgy, Northeastern University, China)
E-mail: zhaoxl@smm.neu.edu.cn

Fabrication of Ti-Ta binary alloy for surgical implant by powder metallurgy

Present research aimed to develop novel Ti-Ta beta alloys for an objective to replace the classical Ti-6Al-4V alloy in surgical implants owing to its better biocompatibility. Alloys with various concentrations of Ta were prepared by powder metallurgy process. Microstructure and the mechanical properties of these alloys were investigated by using various methods.

The Ti-Ta beta alloys were developed aiming the replacement of the classical Ti-6Al-4V alloy in surgical implants owing to its better biocompatibility. Samples of these alloys were obtained following a powder metallurgy (PM) process: blending elemental powders, cold isostatic pressing at 180 MPa for 2h and a sintering process of the compacts for 2h in the range from 1250 to 1500 0C with a heating rate of 20 0C min-1. Then the alloys were characterized by optical microscopy (OM), scanning electron microscopy (SEM), X-ray diffractory, tensile test and dynamic elastic modulus test. Results indicate that the homogenization of the alloy is diffusion-controlled. Besides, the ultimate tensile strength of Ti-Ta products is greatly affected by the variation of temperature and composition: the specimen sintered at 1400 ^{0}C shows the peak value as 917 MPa, and an increase in Ta content leads to a decline. So it is the trend with elastic modulus. It is worth mentioning that the PM products have a much higher ultimate tensile strength and lower elastic modulus than the conventional cast Ti-Ta alloys. A finer grain size and tantalum's solution strengthening may be accounted for the improvement in mechanical strength. The reduction in elastic modulus is closely related to the existence of pores, and a quantified model was conducted to reveal the correlation between porosity and elastic modulus. It has indicated that the Ti-Ta alloys prepared by powder metallurgy process have the great potential for biomedical applications.

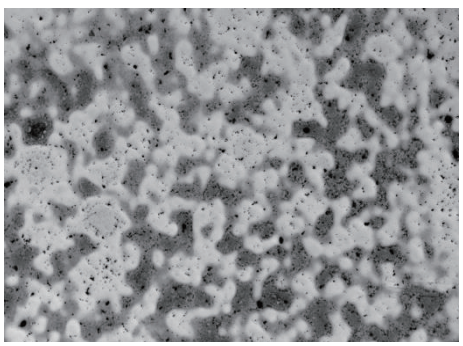

Fig.1 An OM image of typical diffusion-controlled two region structure for Ti-30Ta alloy sintered at 1400 ^{0}C.

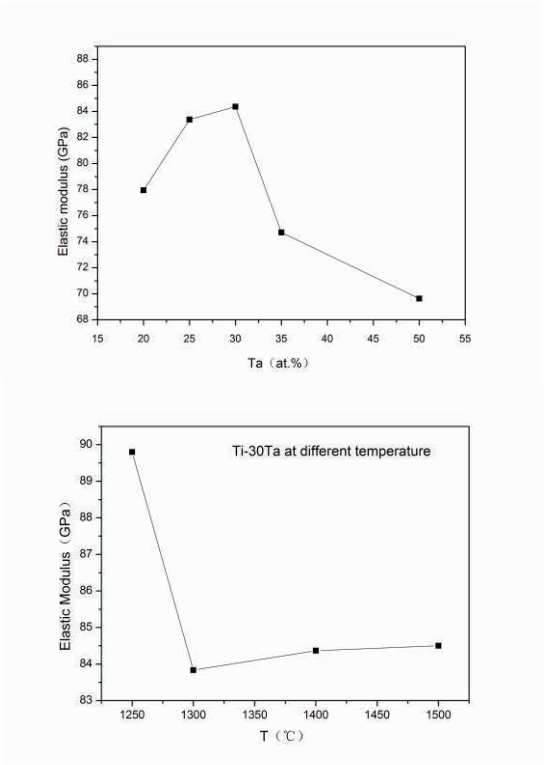

Fig.2 Variation in elastic modulus with sintering temperature and Ta content

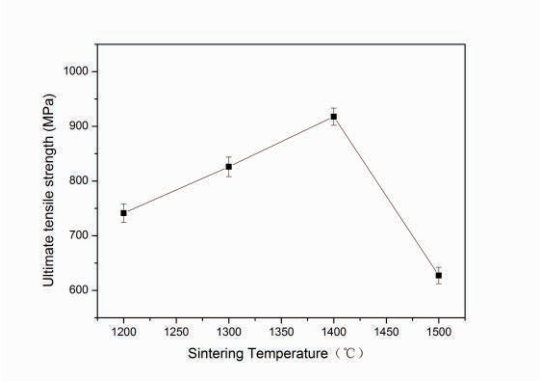

Fig.3 Variation of ultimate tensile strength with sintering temperature for T-30Ta alloy.

Keywords: powder metallurgy, scanning electron microscopy, Young's Modulus,
Hong Wu, State Key Lab for Powder Metallurgy, Central South University
Akihiko Chiba, Materials Processing, Institute for Materials Research, Tohoku University
E-mail: wuhong927@gmail.com, a.chiba@imr.tohoku.ac.jp
http://www.csu.edu.cn; http://www.chibalab.imr.ac.jp/ index.html

Advanced Microstructural Characterization of New Radiation Induced Defects in Reactor Pressure Vessel (RPV) Steels

Two types of radiation-induced defect features, namely unstable matrix damage (UMD) and late-blooming phases (LBP) in RPV steels, which need to be accounted for in more accurate embrittlement prediction, were examined in detail by positron annihilation and atom-probe tomography including recovery anneal. The UMDs involving mono-vacancy equivalent open volume formed faster at higher flux in low Cu steel. LBPs are Ni-Mn-Si precipitates that formed even in low Cu 0.8Ni steel to the volume fraction of 0.16% at 2.1x10^{20} n/cm^2 fluence.

The current prediction model of irradiation hardening and embrittlement of RPV steels under-predicts brittle to ductile transition temperature shift (TTS) of steels irradiated in test reactors to high neutron fluence (ϕt) [1]. Previous studies suggest that this is due to: 1) UMDs formed in aged displacement cascades, that anneal continuously during reactor operation, but build up at high flux (ϕ) in test reactors; and/or 2) late blooming Mn-Ni-Si phases (LBP), that have long been predicted but recently found to grow to very high volume fractions at very high ϕt even in low Cu steels[1].

Accurate prediction of long-term RPV embrittlement requires properly accounting for these types of defects. Hence, the objective of this study is to clarify the character and behavior of UMD and LBP in detail as a function of irradiation and material variables.

14 model RPV steels with systematic chemistry variation were irradiated in BR2 test reactor to two ϕt ≈ 1 and 2.1x10^{20} n/cm^2 at ϕ = 2.3x10^{13} n/cm^{2}s and 290°C. Positron annihilation spectroscopy (PAS) and micro-hardness measurements have been performed before and after a UMD recovery anneal (PIA) at 350°C for 5 h. PAS was also performed on a subset of alloys irradiated at other ϕ=10^{12} and 10^{14} n/cm^{2}s conditions. Atom Probe Tomography (APT) was carried out on selected alloys at ϕt = 2.1x10^{20} n/cm^2.

Figure 1 shows average positron lifetime (τ_{av}) for low and high Cu steels as a function of ϕt at ϕ ≈ 10^{12}, 2x10^{13} and 10^{14} n/cm^{2}s before and after the recovery anneal. Mono vacancy size open volume type defects are indicated by longer τ_{av} that significantly increases with ϕt at ϕ ≥ 2x10^{13}. These features mostly recover during PIA with corresponding τ_{av} similar to a low ϕ=10^{12} n/cm^{2}s condition. Further acceleration of UMD formation by ϕ for ≥ 2x10^{13} n/cm^{2}s is only significant in the low Cu, but not in high Cu steels.

Figure 2 shows APT atom maps indicating formation of Ni-Mn-Si rich LBPs in two no Cu steels with a) 0.8% and b) 1.6% Ni. The respective precipitate volume fractions are 0.16% and 0.47%. The respective average precipitate sizes and number densities are ≈ 2.4 nm/2.3 x10^{23}m^{-3} and ≈ 2.4nm/6.3x10^{23}m^{-3}. The estimated precipitate hardening values are reasonably consistent with the measured extra hardening in these alloys compared to the current EONY model. The hardening model uses the obstacle strength factors obtained in recent UCSB study[2] for well developed LBPs in RPV steels irradiated to much higher ϕt=1x10^{21} n/cm^2.

These data and insights are being used to develop new, physically-based models of embrittlement.

References

[1] G.R.Odette and R.K.Nanstad, JOM 61 (2009) 17
[2] P.Wells, T.Yamamoto, G.R.Odette et al., Acta Mater. accepted.

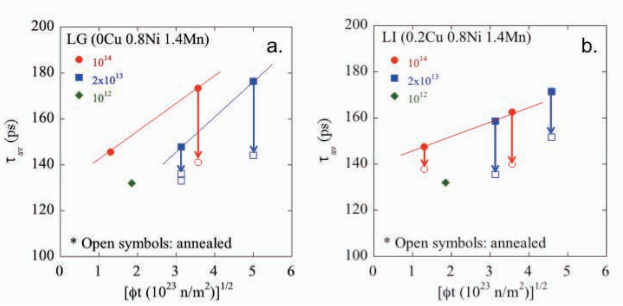

Figure 1 Average positron lifetime (τ_{av}) before (filled) and after (unfilled) recovery anneal versus neutron fluence (ϕt) for ϕ from 10^{12} to 10^{14}n/cm^2 in a) low and b) high Cu RPV steels.

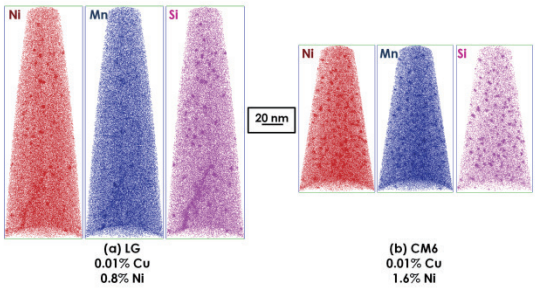

Figure 2 Elemental maps obtained in APT measurements showing formation of Ni-Mn-Si LBP in low Cu steels with a) 0.8%Ni and b) 1.6%Ni

Keywords: nuclear materials, radiation effects, positron annihilation
Takuya Yamamoto (Univ. California Santa Barbara)
Collaborators: Peter Wells, G. Robert Odette (UCSB), Takeshi Toyama, Yasuyoshi Nagai (Tohoku U.)
E-mail: yamataku@engineering.ucsb.edu

Strain response of GdBCO CC tapes with high critical current, I_c under magnetic field (B//c-axis)

Nowadays, REBCO CC tapes have received much attention on applications under magnetic field due to its low magnetic susceptibility. The critical current density, J_c of CC tapes has been enhanced by adopting textured substrate material which gives good buffer and GdBCO layer grain alignment. To predict the behavior of the CC tape and have a good application design (i.e. superconducting motors and generators, SMES etc.), investigating the electromechanical property response of these CC tapes under magnetic field is the first thing to be done.

In this study, two commercially available GdBCO CC tapes fabricated by reactive co-evaporation by deposition and reaction (RCE-DR) process were investigated. However, both CC tape samples have different substrate materials and thicker GdBCO superconducting film adopted. Table 1. shows the specifications of both CC tape samples in details.

Table 1. Properties of GdBCO CC tape samples

Fabrication process	IBAD RCE-DR	
Structure	Ag/GdBCO/$LaMnO_3$/IBAD $MgO/Y_2O_3/Al_2O_3$/substrate	
Superconductor	**GdBCO (~2 μm)**	
Critical current, Ic	> 200 A	
Dimension, t x w	0.194 x 4.18	0.235 x 4.15
Substrate	Hastelloy C-276 (~ 65 μm)	Stainless steel (~100 μm)
Stabilizer	Copper (~15 μm)	
Laminate	Brass (~50 μm	
manufacturer	SuNAM	

Electromechanical property of the CC tape samples was investigated under external magnetic field using the Katagiri-type loading fixture. The fixture was located at the high field laboratory superconducting magnet (HFLSM), Institute of Material Research (IMR) Tohoku University, Japan [1]. It features a loading scheme where the surface of the samples was held perpendicular to the direction of the magnetic field (B//c-axis) produced by 10 T cryocooled superconducting magnet as described elsewhere [**1**]. Length of the sample was 40 mm which includes a 10 mm grip part on both sides (lengthwise). Critical current, I_c was measured using a voltage tap separation of 10 mm and voltage criterion of 1 μV/cm. Strain was monitored by using the dual measurement scheme where two strain gauges (three-wired) are attached on both sides of the CC tape sample while a 15 mm Nyilas-type double extensometer was also installed.

As a result, similar with the one reported else-

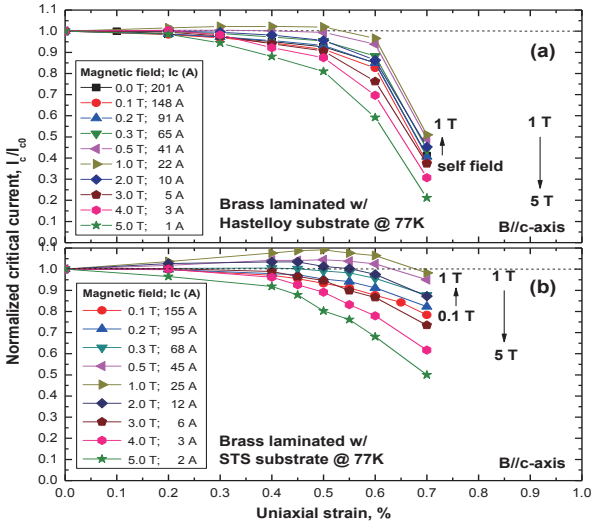

Fig.1. Normalized high critical current, I_c/I_{c0} strain dependence under external magnetic field in RCE-DR CC tapes adopting (a) Hastelloy and (b) Stainless steel substrate.

Where [2], the normalized critical current, I_c/I_{c0}-strain curves of both CC tape samples with different substrate material improved initially with increasing magnetic field up to 1 T indicating an improved strain sensitivity as shown in Fig.1. It can be observed that at 1 T, there is no sign of significant I_c/I_{c0} degradation. However, at 0.5 % strain both CC tape showed I_c peak behavior. By increasing the strain beyond 0.5 %, I_c/I_{c0} significantly dropped but the strain sensitivity of the I_c/I_{c0} curve gradually increased with increasing magnetic field up to 5 T.

As a summary, GdBCO CC tapes with different substrate and relatively high I_c due to the increased GdBCO superconducting layer thickness were significantly affected by strain under external magnetic field.

References

[1] H. S. Shin, M. J. Dedicatoria, S. Awaji, K. Watanabe, IEEE Trans. Appl. Supercond. **22** 6600404 (2012).

[2] H.S. Shin, M.J. Dedicatoria, A. Gorospe, T. Suwa, H. Oguro, and S. Awaji, IEEE Trans. Appl. Supercond. 23 8400404 (2013)

Keywords: superconducting, high field

Hyung-Seop Shin, Alking B. Gorospe, Arman Ray N. Nisay (Andong National University), Hidetoshi Oguro, Satoshi Awaji and Kazuo Watanabe (IMR Tohoku University)
E-mail: hssin@anu.ac.kr, awaji@imr.tohoku.ac.jp
http://www.andong.ac.kr/

Activity Report

Young Researcher Fellowships

FY 2013 Young Researcher Fellowships

No.	Name	Host	Proposed Research	Title	Affiliation	Term
13FS1	Jaroslav Valenta	F. Honda	Effect of Pressure on the Electronic State of RCo2 (R:Rare-Earth) Ferrimagnets	Ph. D. Student	Charles University, Czech	2014.1.25-3.1
13FS2	Irina Stockem	H. Nojiri	Theoretical Investigation of the Spin Dynamics in the Pt/Co/a-Cr203 Thin Film Systems	Ph. D. Student	University of Applied Sciences Bielefeld	2014.3.2-3.8

Electronic state of RCo_2 (R: rare-earth) ferrimagnets under high pressure

Recently, high pressure techniques become indispensible in the field of solid state physics and materials science for better understanding of electronic structures of materials. In order to clarify the origin of "pari"-magnetism, we have performed electrical resistivity experiments on $HoCo_2$ single crystal under high pressure.

$HoCo_2$ belongs to a group of intermetallic RCo_2 (R = rare earth) compounds forming a cubic Laves phase ($MgCu_2$-type, space group *Fd-3m*). Localized 4*f* magnetic moments of R element coexist together with the itinerant Co 3*d* moments in RCo_2 compounds. Both magnetic sublattices (R and Co) align antiparallel for heavy rare-earths (Gd, Tb, etc.) below Curie temperature T_C. The magnetic moment of Co appears on the verge of magnetism. Recently, it is found that there is a short-range magnetic correlation between 4*f* and 3*d* moments even above T_C, which is called "*parimagnetism*" [1]. In order to clarify the origin of parimagnetism, we have carried out electrical resistivity measurements on $HoCo_2$ under high pressure.

The single crystalline sample of $HoCo_2$ was grown by flux method. The magnetic transition temperatures on the studied single crystal are checked by Physical Property Measurement System in laboratory for α-emitters in Sendai. High pressure was generated using Bridgman anvil type pressure apparatus. Pressure inside the cell was calibrated by the superconducting transition of lead. Daphne 7373 was used as pressure transmitting medium. Fig.1 shows the temperature dependence of the electrical resistivity on $HoCo_2$ under high pressure.

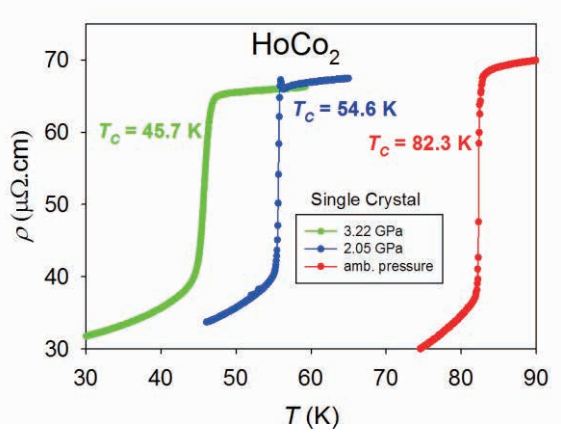

Fig. 1 Temperature dependence of electrical resistivity measured on $HoCo_2$ single crystal.

The pressure evolution of T_C on $HoCo_2$ shows rapid decrease of T_C up to 3.22 GPa and for $P > 4$ GPa T_C is nearly pressure independent which is in good agreement with the data obtained by polycrystalline sample [2], as shown in Fig. 2. On the other hand, the magnetic reorientation temperature T_R, where the easy direction of magnetization changes from the [100] to [110], slowly increases with increasing pressure.

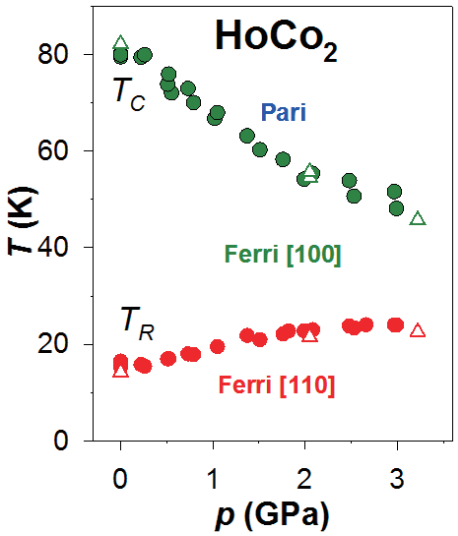

Fig. 2 Obtained *T-P* magnetic phase diagram of $HoCo_2$. Open symbols are obtained by the present study.

This project's impact is extending of the pressure range for the measured data on the studied RCo_2 compounds and considerable is also a great experience of a young scientist with high level pressure equipment in the IMR laboratory.

References

[1] F. Bartolomé *et al.*, Eur. Phys. J. B, **86** (2013) 489.
[2] O. Syshchenko, *et al.*, *J. Alloys and Compd.* **317-318** (2001) 438.

Keywords: RCo_2, "pari"-magnetism, high pressure
Jaroslav Valenta (DCMP, Charles University in Prague), Fuminori HONDA (Actinide Materials Science)
E-mail: valeja@mag.mff.cuni.cz , honda@imr.tohoku.ac.jp
http://www-lab.imr.tohoku.ac.jp/~aokilab/index.html

Investigation of the magnetization dynamics of the Pt/Co/a-Cr_2O_3 thin film system by atomistic spin dynamics methods

We investigated the perpendicular exchange bias system Pt/Co/a-Cr_2O_3 by means of classical spin dynamics simulations. First, we studied a simplified four macro-spin system, where two macro-spins model a ferromagnetic and an antiferromagnetic layer, resp. In our next approach we have modeled the Co and Cr_2O_3 layers of the system by taking into account the true microscopic structure. We have obtained first results for the interlayer exchange coupling, ground states and the resulting switching behavior.

In spin valves the giant magneto resistance (GMR) depends on the relative orientation of two ferromagnetic layers. To change the resistance, one of the layers has to possess a fixed orientation of the magnetization in a certain magnetic field range, while the other is free and can be controlled by an external field.
While the magnetization curve of a pure ferromagnetic is symmetric along the magnetization axes, the system consisting of a free and a fixed layer shows a shift of the magnetization curve, the so called exchange bias.
A multilayer system showing perpendicular exchange bias (PEB) has been investigated by Y. Shiratsuchi *et al.* [1], [2]. The perpendicular orientation of a ferromagnetic Pt/Co film is fixed due to the interfacial exchange coupling to the antiferromagnetic Cr_2O_3.

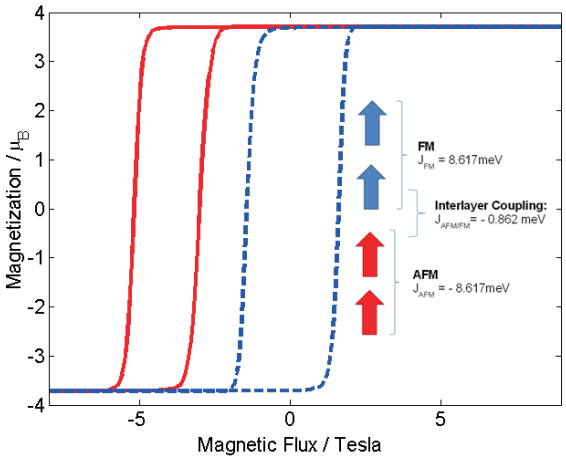

Fig. 1Magnetization curves of simplified 4 spin system without interlayer interaction (blue dashed line) and with antiferromagnetic interlayer interaction (red line).

As a first approach we studied a simplified model consisting of a chain of four macro-spins where two macro-spins represent a ferromagnetic layer and the two other macro-spins represent an antiferromagnetic layer (see Fig. 1). Taking into account only the classical Heisenberg exchange coupling, a small interlayer coupling and the Zeeman-term, the exchange bias effect is already visible without introducing additional anisotropies. To determine the interfacial exchange coupling and its effect on the switching behavior, we have created a microscopic model of a system consisting of a Co(111) thin film superposed on Cr_2O_3(0001) and studied the magnetic properties by classical spin dynamics simulations.

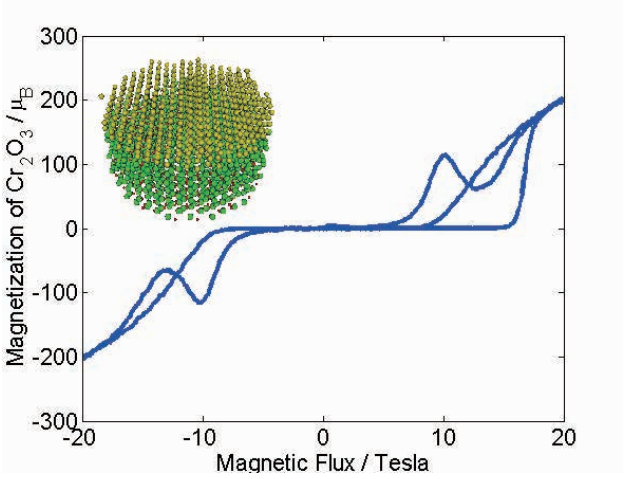

Fig. 2 Simulation of the dynamical hysteresis of Cr_2O_3 in the Pt/Co/a-Cr_2O_3 system with 430 µeV interlayer exchange interaction.

In order to determine the interlayer exchange coupling, our simulated magnetization curves (see Fig. 2) will be compared to experimental data in a future work.

References

[1] Y. Shiratsuchi et al., Appl. Phys. Express 3, 113001 (2010).
[2] Y. Shiratsuchi et al., Appl. Phys. Lett. 100, 262413 (2012).

Keywords: thin films, magnetoresistance (magnetic), simulation
Irina Stockem (Bielefeld University of Applied Sciences)
E-mail: Irina.Stockem@fh-bielefeld.de
http://www.fh-bielefeld.de

ICC-IMR FY2013
Activity Report

Edited by ICC-IMR Office
Published in February, 2018

Contact: International Collaboration Center,
Institute for Materials Research (ICC-IMR)
Tohoku University
2-1-1, Aoba-ku, Sendai, 980-8577, Japan
TEL&FAX: 81-22-215-2019
E-mail: icc-imr@imr.tohoku.ac.jp

Printing: HOKUTO Corporation

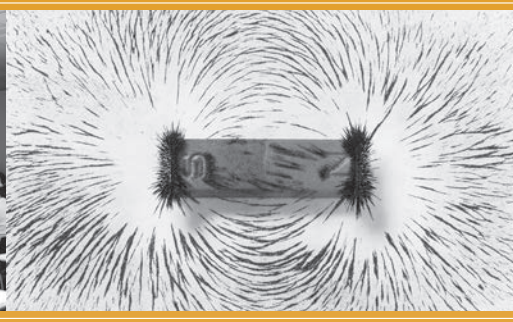

この冊子は「水なし印刷」により印刷しております。

環境にやさしい植物油インキ「VEGETABLE OIL INK」で印刷しております。